NJC

Accepted Manuscript

This is an *Accepted Manuscript*, which has been through the Royal Society of Chemistry peer review process and has been accepted for publication.

Accepted Manuscripts are published online shortly after acceptance, before technical editing, formatting and proof reading. Using this free service, authors can make their results available to the community, in citable form, before we publish the edited article. We will replace this *Accepted Manuscript* with the edited and formatted *Advance Article* as soon as it is available.

You can find more information about *Accepted Manuscripts* in the Information for Authors.

Please note that technical editing may introduce minor changes to the text and/or graphics, which may alter content. The journal's standard Terms & Conditions and the Ethical guidelines still apply. In no event shall the Royal Society of Chemistry be held responsible for any errors or omissions in this *Accepted Manuscript* or any consequences arising from the use of any information it contains.

ROYAL SOCIETY OF CHEMISTRY

www.rsc.org/njc

NJC

RSCPublishing

LETTER

Biogenic silver nanoparticles impregnated hollow mesoporous silicalite-1: An efficient catalyst for p-nitrophenol reduction

Cite this: DOI: 10.1039/c3njoooooox

Rituparna Das,[a] Sourav Ghosh,[a] Ipsita Hazra Chowdhury [a] and Milan Kanti Naskar[a]*

Received ooth XXXXX 2013,
Accepted ooth XXXXX 2013

DOI: 10.1039/c3njoooooox

www.rsc.org/njc

AgNPs impregnated hollow mesoporous silicalite-1 was synthesized using green *carambola* extract. The AgNPs of size 10-15 nm were well dispersed mostly within the shell of hollow silicalite-1 which contained hierarchical porosity. The synthesized product showed enhanced catalytic efficiency for the reduction of p-nitrophenol.

Silver nanoparticles (AgNPs) are currently the focus of **intense** research interest due to their unique characteristics such as low toxicity, biocompatibility, antimicrobial activity, optoelectronic, cryogenic superconducting, biosensing and catalytic properties.[1,2] The intrinsic properties of AgNPs are determined by their size, shape, crystallinity, structure (solid or hollow) and surface functionality.[3,4] The AgNPs are commonly synthesized by wet-chemical reduction of silver ions **in the presence of** reducing agents. However, the particles synthesized by conventional method are agglomerated **in the** form clusters or even large particles. Biosynthesis of AgNPs using plant-based extracts has drawn a remarkable research interest because they can act as reducing agents as well as capping agents following an environmentally friendly, sustainable and cost effective process. Recently, we have synthesized water dispersible AgNPs using aqueous extract of *Carambola* fruit following a simple room temperature procedure.[5] For catalytic applications of AgNPs, the catalysts are dispersed **in** an inorganic matrix (support) to improve their functionality by reducing aggregation and stabilization of the nanoparticles.[6]

Zeolite as catalyst **support** has attracted interest because of **its** high thermal and mechanical stability, and unique shape selectivity. However, the presence of microporosity in zeolite could retard the catalytic activity. Introduction of mesoporosity in zeolite structure can facilitate high dispersion of the catalyst, and also shortening the diffusion path to enhance the catalytic performance. Hollow mesoporous zeolites, in particular are the most promising candidates as catalytic support due to their high surface area and high inertness under harsh condition. One of the existing methods of preparing hollow zeolite spheres is the layer-by-layer assembly technique.[7,8] Hollow zeolites are also prepared by leaching technique with alkali treatment.[9-11] Dong *et al.*[12] prepared hollow silicalite-1 spheres by vapour-phase transport (VPT) treatment. Mesoporous zeolites have been synthesized by soft templating route using cationic or silylated polymer and amphiphilic organosilane as template,[13] hard templating route,[14,15] and non-templating route involving desilication-dealumination by alkali leaching technique.[16]

In the present **study,** we have synthesized AgNPs impregnated hollow mesoporous silicalite-1 using green ***carambola*** extract, the first time we report, to the best of our knowledge. Catalytic reduction of p-nitrophenol (4-NP) to p-aminophenol (4-AP) has been investigated with the synthesized products. The 4-NP is a water-pollutant present in industrial effluents, while 4-AP is used in drug industry, photographic developer, corrosion inhibitor etc. Here, the AgNPs impregnated hollow mesoporous silicalite-1 showed enhanced catalytic efficiency with faster **reaction** (rate constant 5.5×10^{-3} s^{-1}), and can be reused several times without any significant **changes in** their original catalytic activity.

AgNPs impregnated hollow mesoporous silicalite-1 was synthesized hydrothermally at 170°C/72h followed by alkali treatment, and impregnation with biogenic AgNPs; the products were characterized by different techniques (Experimental section, ESI). The catalytic performance of the products for the reduction of 4-NP was also studied (Catalytic performance, ESI). The parent silicalite-1 (S-1) crystals synthesized hydrothermally at 170°C/72h were hexagonal **in shape** with the size range of 400-800 nm (Fig. S1a,b, ESI). After alkali treatment with 0.2 M tetrapropyl ammonium hydroxide (TPAOH), a void was created in the interior of the silicalite-1 (HS-1) crystals (Fig. S1c,d, ESI). **The TEM images (Fig. S2a,b, ESI) show** the hexagonal shaped solid and void crystals before and after alkali treatment, respectively. During desilication process by alkali treatment, the surface Si-OH groups of crystals **loose** proton rendering negatively charged Si-O^-. These Si-O^- ions interact with TPA^+ ions, which reduce dissolution of external surface of silicalite-1. However, silicate oligomers are leached from the interior of the crystal, where crystallization is yet to **be completed**. The leached silicate oligomers interact with TPA^+ **ions** on the silicalite-1 surface forming silicate/TPA intermediate state, and recrystallize at 170°C. Thus, continued desilcation and recrystallization resulted in the formation of hollow silicalite-1 crystals. Figure 1 shows (a,b) the FESEM and (c,d) TEM images of AgNPs impregnated hollow silicalite-1 (Ag-HS-1). It is to be noted that the hollowness of all particles **was** not uniform (TEM image in Fig. S3, ESI shows the particles with thicker shell compared to the particle shown in Fig. 1c).

In the impregnation process (at pH 10), the polysaccharide (polyols) and ascorbic acid ($C_6H_8O_6$) present in *Carambola* fruit extract facilitate in the formation of AgNPs from Ag^+ ions. In alkaline pH, the capping and stabilizing ability of bio molecules

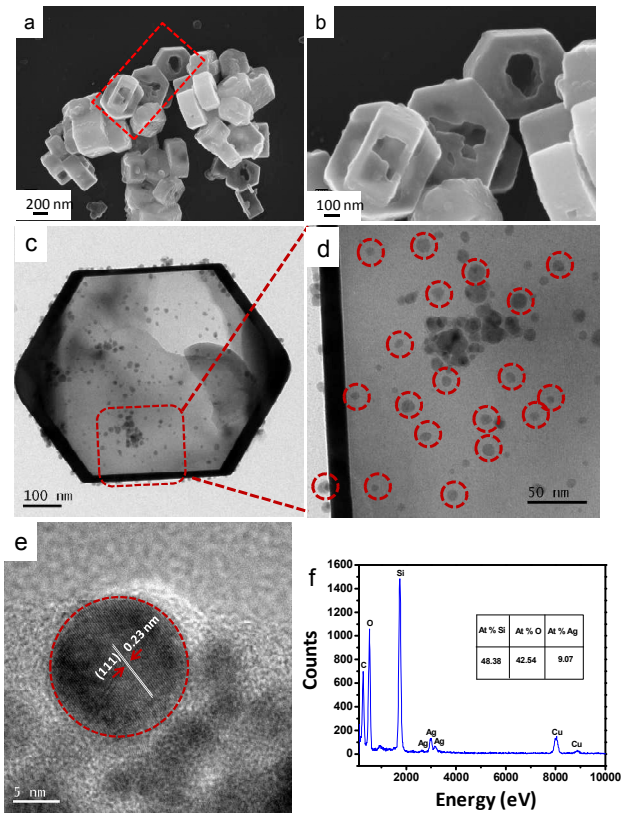

Fig.1: (a,b) FESEM, (c,d) TEM, (e) HRTEM and (f) EDS of AgNPs impregnated hollow silicalite-1

become higher due to repulsion of electrical charge particles to stabilize AgNPs with smaller sizes. TEM image (Fig. 1c,d) reveals that AgNPs of size 10-15 nm **were** dispersed mostly within the shell of hollow silicalite-1. The HRTEM image (Fig. 1e) of AgNPs impregnated sample shows the d-spacing of 0.23 nm corresponding to (111) plane of Ag indicating the presence of Ag nanoparticles (shown in dotted circle). The energy dispersive X-ray spectroscopy (EDS) (Fig. 1f) determined **the presence** of about 9% Ag atom in the sample. The oxidation state of Ag in AgNPs impregnated silicalite-1 was determined by X-ray photoelectron spectroscopy (Fig. S4, ESI). The spectral profile reveals two peaks at 367.6 and 373.6 eV **which corresponded** to $Ag3d_{5/2}$ and $Ag3d_{3/2}$, respectively. It indicated characteristic of metallic silver (Ag^o) in the sample.[17] Figure 2 shows (a) XRD pattern and (b) FTIR of AgNPs impregnated hollow silicalite-1.

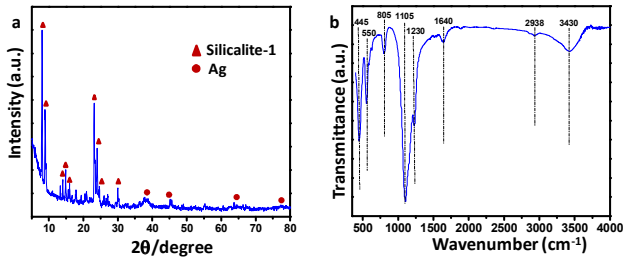

Fig. 2: (a) XRD pattern and (b) FTIR of AgNPs impregnated hollow silicalite-1

In the XRD patterns, crystallization of silicalite-1 **along with** metallic Ag (JCPDS No. 04-0783) **was revealed. The characteristic peaks of metallic Ag appeared** at 2θ values of around 38.01°, 44.26°, 64.02° and 77.36° corroborating to the crystal planes of [111], [200], [220] and [311], respectively. The characteristic peaks of parent and hollow silicalite-1 are also exhibited in Fig. S5 (ESI).[18] The FTIR spectra (Fig. 2b) of the samples **show** an intense pentasil vibration **at 550 cm^{-1}** of silicalite-1. The appearance of absorption bands at 445 and 805 cm^{-1} corroborated to Si-O-Si rocking and symmetric stretching and bending vibrations, respectively. The internal and external asymmetric stretching modes of vibrations are observed at 1105 and 1230 cm^{-1}, respectively.[19] Interestingly, the presence of absorption band at 1640 cm^{-1} indicated that polyols in carambola extract got oxidized to unsaturated carbonyl groups[20] rendering reduction of Ag^+ to metallic Ag. The weak band at 2938 cm^{-1} was the characteristic C-H stretching vibration of ascorbic acid present in carambola extract, while O-H stretching vibration of absorbed water shows the band at 3430 cm^{-1}. The characteristic FTIR spectra of parent and hollow silicalite-1 are shown in Fig. S6 (ESI). Figure 3 shows (a) N_2 adsorption-desorption isotherms, and pore size distributions (PSD) by (b) DFT and (c) BJH methods for AgNPs impregnated hollow silicalite-1 sample.

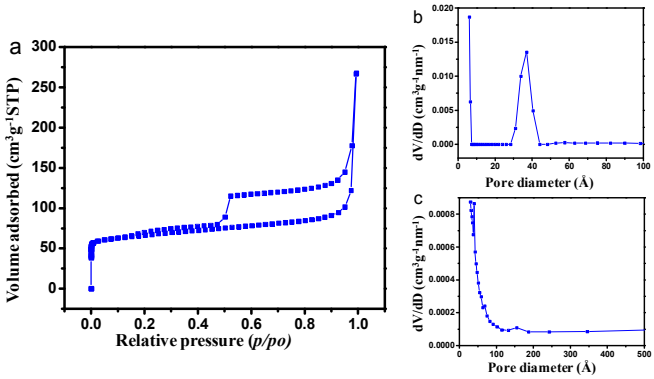

Fig. 3: (a) N_2 adsorption-desorption isotherms, and pore size distributions (PSD) by (b) DFT and (c) BJH methods of AgNPs impregnated hollow silicalite-1

The N_2 adsorption-desorption isotherms **show** the presence of H2 hysteresis loop with an abrupt steep around p/p_o = 0.5 in the desorption branch. The presence of microporosity and mesoporosity in the sample was confirmed by PSD curves determined by DFT (Fig. 3b) and BJH (Fig. 3c) methods, respectively. The TEM image (Fig. S7, ESI) also confirmed the presence of mesoporosity (marked as circle) in the sample. The BET isotherms and PSDs of the parent and hollow silicalite-1 are revealed in Figs. S8 and S9 (ESI), respectively. For the parent silicalite-1 sample, a steep rise in the isotherm occurred at lower relative pressure, around p/p_o = 0.1, which indicated abundance of microporosty in the samples. However, the isotherms with two hysteresis loops for hollow silicalite-1 show a small loop at around p/p_o = 0.1 and a large loop at around p/p_o = 0.5**,** reflecting both the microporosity and meso/macro porosity, respectively in the samples. Such isotherms are very unusual demonstrating existence of two different types of pore systems with narrow pore size distribution.[21] It can be concluded that the hysteresis loops at the p/p_o = 0.5 resulted due to dissolution of silica with 0.2 M TPAOH treatment. With the impregnation of AgNPs in hollow silicalite-1, the hollow structure was preserved in the presence of micro and mesoporosity of the samples, which was reflected in the same nature of isotherms in both the hollow silicalite-1 and AgNPs impregnated hollow silicalite-1 samples. The

textural properties of parent (S-1), hollow silicalite-1 (HS-1) and AgNPs impregnated hollow silicalite-1 (Ag-HS-1) are shown in Table 1.

Table 1: The textural properties of S-1, HS-1 and Ag-HS-1

Sample ID	S_{BET} (m^2g^{-1})[a]	$S_{Micropore}$ (m^2g^{-1})[b]	$S_{External}$ (m^2g^{-1})[c]	$V_{p\text{-}Total}$ (cm^3g^{-1})[d]	d_p (nm)[e]
S-1	351	297	54	0.228	2.6
HS-1	301	181	120	0.422	5.6
Ag-HS-1	241	119	122	0.415	6.9

[a]BET surface area; [b]micropore surface area; [c]external surface area; [d]total pore volume; [e]average pore size

It **exhibits** that BET surface area and microporous surface area decreased in the order of S-1> HS-1 > Ag-HS-1. It is mentioned worthy that the BET surface area is the total specific surface area measured by BET method. The micrporous surface area is obtained by the difference between BET surface area and the external surface area i.e, mesoporous surface area (derived from the slope of the t (statistical thickness)-plot).[22] For microporous materials like silicalite-1, the linear BET region occurs at p/p_o < 0.1, while the linear t-plot range is obtained at higher p/p_o. Significant reduction of total surface area along with microporous surface area, and increment of mesoporous surface area (external surface area) from S-1 to HS-1 (Table 1) could be due to the structural distortion.[23] It could occur during desilication followed by second calcination step. The decrease in microporous surface area from HS-1 to Ag-HS-1 could be attributed to the partial filling of micropores during impregnation of AgNPs. It was evidenced by the closer hysteresis loop at p/p_o < 0.5 (Fig. 3a). Interestingly, the average pore size also significantly increased after desilication of silicalite-1. Furthermore, for the AgNPs impregnated hollow silicalite-1 sample, the increase in average pore diameter and reduction of surface area were attributed to development of partial strain generated during incorporation of AgNPs.[24] Compared to S-1, the increase in total pore volume in HS-1 and Ag-HS-1 was due to the presence of higher mesoporosty in the latter samples.

The catalytic performance of AgNPs impregnated silicalite-1 was evaluated by the reduction of 4-NP to 4-AP using $NaBH_4$ under ambient conditions. The UV-Vis spectra (Fig. 4a) of the sample reveal that with increase in time of catalytic reaction, the absorbance at 400 nm of 4-NP was reduced and the concomitant increase of 4-AP absorption peak at 296 nm**.** The reaction was almost completed within 6 min. The reducing activity of $NaBH_4$ was checked in the absence of Ag-HS-1 catalyst (blank experiment). The UV-Vis **absorptions** of 4-NP, 4-NP+$NaBH_4$ (at 0 min) and 4-NP+$NaBH_4$ (after 30 min) **depict** (Fig. S10, ESI) that the absorption peaks at 317 nm of 4-NP shifted to 400 nm in the presence of $NaBH_4$, which was remained almost unchanged even after 30 min of absorption. It is to be noted that in the absence of catalyst **(Ag-HS-1)**, no characteristic peak at 296 nm appeared for the reduction of 4-NP to 4-AP. It could be explained that the high kinetic barrier between mutually repelling negative ions of 4-NP and BH_4^- **inhibits** the further reduction of 4-NP[25] in the absence of Ag-HS-1 catalyst. Figure 4b shows the logarithm plot of the absorbance ($-\ln A_t/A_o$) with reaction time. It reveals pseudo first order reaction, and the apparent rate constant **(k)** was calculated **as** 5.5×10^{-3} s^{-1} (0.33 min^{-1}). The activity parameter κ (rate constant per unit mass of Ag) of the catalyst was calculated as 65.63 $s^{-1}g^{-1}$, which was found to be higher than reported literature (Table S1).[26-29] It demonstrates that AgNPs impregnated hollow

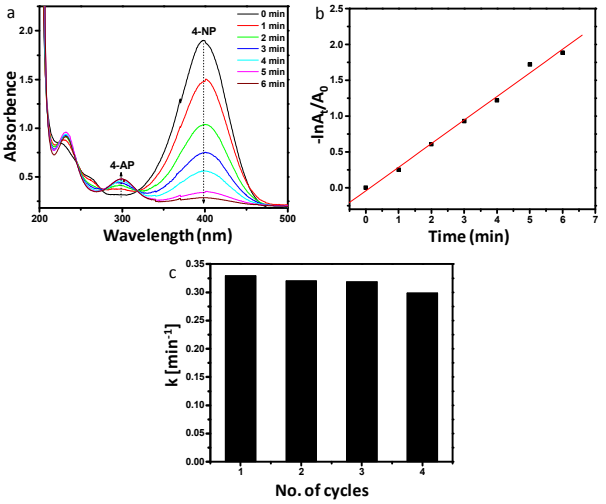

Fig. 4: (a) UV-Vis absorption spectra for the reduction of 4-NP to 4-AP in presence of AgNPs impregnated hollow silicalite-1 particles; (b) pseudo first order plot of -ln A_t/A_0 (absorbance intensity at 400 nm) versus time for above reaction; (c) apparent rate constant values (k) of the above catalytic reduction in four consecutive cycle.

silicalite-1 is advantageous for enhanced catalytic efficiency because of well dispersion of AgNPs in hollow architectures with large surface area.[6] The stability of catalytic efficiency was checked for 4 cycles indicating recyclability of the catalyst (Fig. 4c).

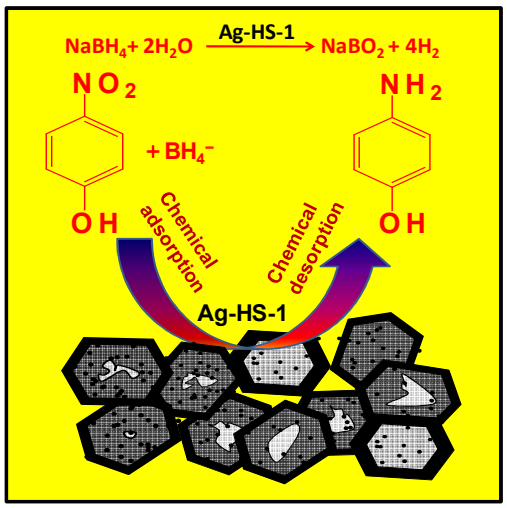

Fig. 5: Schematic representation for catalytic reaction mechanism

The catalytic reaction mechanism for the reduction of 4-NP to 4-AP in the presence of AgNPs impregnated silicalite-1 is shown in Fig. 5. In the reaction mechanism**,** both the donor BH_4^- ions obtained from $NaBH_4$ and the acceptor 4-NP molecules coadsorb on catalyst surface (Ag-HS-1) through chemical adsorption.[30] Here, $NaBH_4$ could transfer hydrogen species **to** catalytic surface (Ag-HS-1) under aqueous condition.[31] In this case, the catalyst **acts** as a hydrogen shuttle, and simultaneous reduction of 4-NP to 4-AP takes place *via* desorption process.

In conclusion, we have firstly reported the synthesis of biogenic AgNPs impregnated hollow mesoporous silicalite-1 using green carambola extract. The AgNPs of size 10-15 nm **were** well

dispersed mostly within the shell of hollow silicalite-1. The AgNPs impregnated hollow silicalite-1 contained hierarchical porosity. The porous product **revealed** enhanced catalytic efficiency for the reduction of 4-NP to 4-AP. We anticipate that the present method can be applicable for other catalytic **activities** by tuning the porosity and the size of Ag and/or other noble and transition metals impregnated hollow zeolite.

Acknowledgement

This research was financially supported by Department of Science and Technology under the DST-SERB sponsored project, GAP 0616 (Grant No. SR/S3/ME/0035/2012), Government of India. RD and IHC are thankful to UGC, and SG is thankful to CSIR for their fellowships.

Notes and references

[a]Sol-Gel Division, CSIR-Central Glass and Ceramic Research Institute, Kolkata 700 032, India
*Corresponding author. E-mail: milan@cgcri.res.in, Fax: +91 33 24730957

Electronic Supplementary Information (ESI) available: [details of **experimental section, catalytic performance, Characterization and** any supplementary information available should be included here]. See DOI: 10.1039/c000000x/

1. G.N.R. Tripathi, *J. Am. Chem. Soc*., 2003, 125, 1178-1179.
2. S.S. Ravi, L.R. Christena, N. Sai Subramanian and S.P. Anthony, *Analyst.*, 2013, 138, 4370-4377.
3. S. Li, Y. Shen, A. Xie, X. Yu, L. Qiu, L. Zhang and Q. Zhang, *Green Chem.*, 2007 9, 852-858.
4. B.L. Devi and A.B. Mandal, *RSC Adv.,* 2013, 3, 5238-5253.
5. I.H. Chowdhury, S. Ghosh, M. Roy and M.K. Naskar, *J. Sol-Gel Sci. Technol*., 2015, 73, 199-207.
6. Z. Niu, S. Zhang, Y. Sun, S. Gai, F. He, Y. Dai, L. Li and P. Yang, *Dalton Trans*., 2014, 43, 16911-16918.
7. K.H. Rhodes, S.A. Davis, F. Caruso, B.J. Zhang and S. Mann, *Chem. Mater*., 2000, 12, 2832-2834.
8. V. Valtchev and S. Mintova, *Micropor. Mesopor. Mater.,* 2001, 43, 41-49.
9. C.S. Mei, Z.C. Liu, P.Y. Wen, Z.K. Xie, W.M. Hua and Z. Gao, *J. Mater. Chem.,* 2008, 18, 3496-3500.
10. C. Dai, A. Zhang, L. Li, K. Hou, F. Ding, J. Li, D. Mu, C. Song, M. Liu and X. Guo, *Chem. Mater.,* 2013, 25, 4197-4205.
11. D. Fodor, L. Pacosova, F. Krumeich and J.A. van Bokhoven, Chem. Commun., 2014, 50, 76-78.
12. A. Dong, Y. Wang, Y. Tang, N. Ren, Y. Zhang and Z. Gao, *Chem. Mater*., 2002, 14, 3217-3219.
13. H. Wang and T.J. Pinnavaia, *Angew. Chem. Int. Ed*., 2006, 45, 7603-7606.
14. W. Fan, M.A. Snyder, S. Kumar, P. S. Lee, W.C. Yoo, A.V. McCormick, R.L. Penn, A. Stein and M. Tsapatsis, *Nat. Mater.,* 2008, 7, 984-991.
15. J-S. Yu, S.B. Yoon, Y.J. Lee and K.B. Yoon, J. Phys. Chem. B, 2005, 109, 7040-7045.
16. J. Perez-Ramirez, S. Abello, A. Bonilla and J.C. Groen, *Adv. Funct. Mater*., 2009, 19, 164-172.
17. S. Nath, S.K. Ghosh, S. Praharaj, S. Panigrahi, S. Basu and T. Pal, *New J. Chem*., 2005, 29, 1527-1534.
18. M.M.J. Treacy and J.B. Higgins in Collection of Simulated XRD Powder Patterns for Zeolite (Elsevier, Amsterdam, 2001).
19. J. Brinker and G.W. Scherer, *Sol-Gel Sci.*: The Physics and Chemistry of Sol-Gel Processing, Academic Press: San Diego, CA, 1990.
20. D. Jain, H.K. Daima, S. Kachhwaha and S.L. Kothari, *Dig. J. Nanomater. Biostruct.*, 2009, 4, 723-727.
21. A. -H. Lu, W. Schmidt, B. Spliethoff and F. Schuth, *Adv. Mater.,* 2003, 15, 1602-1606.
22. D. W. Rutherford, C. T. Chiou and D. D. Eberl, *Clays Clay Miner.,* 1997, 45, 534-543.
23. A. -H. Lu, W. -C. Li, W. Schmidt and F. Schuth, *Micropor. Mesopor. Mater.,* 2005, 80, 117-128.
24. S. M. El-Sheikh, A. A. Ismail and J. F. Al-Sharab, *New. J. Chem.,* 2013, 37, 2399-2407.
25. Z. Dong, X. Le, Y. Liu, C. Dong, J. Ma, J. Mater. Chem. A, 2014, 2, 18775–18785.
26. Y. Liu, Y. Zhang, H. Ding, S. Xu, M. Li, F. Kong, Y. Luo, G. Li, *J. Mater. Chem. A*, 2013, 1, 3362-3371.
27. M. H. Rashid, T. K. Mandal, *J. Phys. Chem. C*, 2007, 111, 16750-16760.
28. S. Tang, S. Vongehr, X. Meng, *J. Mater. Chem.*2010, 20, 5436-5445.
29. A. Gangula, R. Podila, M. Ramakrishna, L. Karanam, C. Janardhana, A. M. Rao, *Langmuir,* 2011, 27, 15268-15274.
30. Z. Jiang, J. Xie, D. Jiang, X Wei and M. Chen, *CrystEngComm*, 2013, 15,560-569.
31. R. Kaur, C. Giordano, M. Gradzielski, S. Mehta, *Chem. Asian J.,* 2014, 9, 189-198.

TOC

Hollow silicalite-1 impregnated with Ag nanoparticles using plant extract shows the excellent catalytic activity for 4-NP reduction.